International Journal of Thermophysics, Vol. 21, No. 4, 2000

Measurements of Thermal Conductivity and Electrical Conductivity of a Single Carbon Fiber

X. Zhang,[1,2] S. Fujiwara,[1] and M. Fujii[1]

Received November 8, 1999

In this paper, the thermal conductivity of a single carbon fiber under different manufacturing conditions is measured using the steady-state short-hot-wire method. This method is based on the heat transfer phenomena of a pin fin attached to a short hot wire. The short hot wire is supplied with a constant direct current to generate a uniform heat flux, and both its ends are connected to lead wires and maintained at the initial temperature. The test fiber is attached as a pin fin to the center position of the hot wire at one end and the other end is connected to a heat sink. One-dimensional steady-state heat conduction along the hot wire and test fiber is assumed, and the basic equations are analytically solved. From the solutions, the relations among the average temperature rise of the hot wire, the heat generation rate, the temperature at the attached end of the fiber, and the heat flux from the hot wire to the fiber are accurately obtained. Based on the relations, the thermal conductivity of the single carbon fiber can be easily estimated when the average temperature rise and the heat generation rate of the hot wire are measured for the same system. Further, the electrical conductivity of the single carbon fiber is measured under the same conditions as for the thermal conductivity using a four-point contact method. The relation between the thermal conductivity and electrical conductivity is further discussed, based on the crystal microstructure.

KEY WORDS: electrical conductivity; microstructure; pin fin; single carbon fiber; steady-state short-hot-wire method; thermal conductivity.

1. INTRODUCTION

Thermal conductivity is one of the most important properties to evaluate the heat transfer characteristics of a fine fiber like carbon fiber [1, 2], metallic and non-metallic fibers [3, 4], etc. Generally, it is very difficult to

[1] Institute of Advanced Material Study, Kyushu University, Kasuga 816-8580, Japan.
[2] To whom correspondence should be addressed.

0195-928X/00/0700-0965$18.00/0

measure the thermal conductivity of such a fine fiber since it has a diameter of 10 μm or less, though a few measurements [5, 6] have been reported. Therefore, the thermal conductivity of a fine fiber is usually estimated from measurements of a composite specimen including a bundle of the fibers. Due to the complicated effects of glue material and composite structure, however, the conventional method [7, 8] sometimes gives thermal conductivity values far from the value for a single fiber. Consequently, a new effective and accurate method to measure the thermal conductivity of a single fine fiber has been developed by Zhang et al. [9–11].

In our previous paper, we had obtained analytical solutions for various measurement conditions and clarified quantitatively the applicability and accuracy of this method. It was found that the thermal conductivity could be measured accurately up to 1000 $W \cdot m^{-1} \cdot K^{-1}$ for a fiber of 10 to 30 μm in diameter. Further, we had conducted preliminary experiments using samples of Pt wire (100.8-μm diameter) and Cu wire (41.7 μm diameter) and confirmed the validity of the present method. The present paper describes the measurements of the thermal conductivity and electrical conductivity of a single carbon fiber at different manufacturing conditions. Based on the standpoint of microstructure, the relation between the thermal conductivity and electrical conductivity is further discussed. Finally, a correlation between them is proposed.

2. PRINCIPLE OF MEASUREMENT

Figure 1 shows schematically the measuring system, the physical model, and the coordinate system for the following theoretical analysis. The hot wire of radius r_h and length l_h is supported with the lead wire at each end and supplied with a constant direct current to generate a uniform heat flux. The test fiber of radius r_f and length l_f is attached to the center position of the hot wire at one end, and the other end is supported with a lead wire as a heat sink. The lengths of the left- and right-hand sides of the hot wire from the attached point are l_{h1} and l_{h2}, respectively. Both ends of the hot wire and the end of the test fiber attached to the heat sink are maintained at the initial temperature during the entire measurement. The system is similar to the heat transfer phenomenon from a pin fin. In the present case, however, due to the low small heat capacity of the hot wire, the base temperature of the fin is greatly affected by the heat transfer characteristics of the fin itself. The temperature at the junction point of the hot wire and test fiber depends on the values of the thermal conductivity of the hot wire λ_h and test fiber λ_f, the heat generation rate of the hot wire, and the heat transfer coefficients around the hot wire and test fiber.

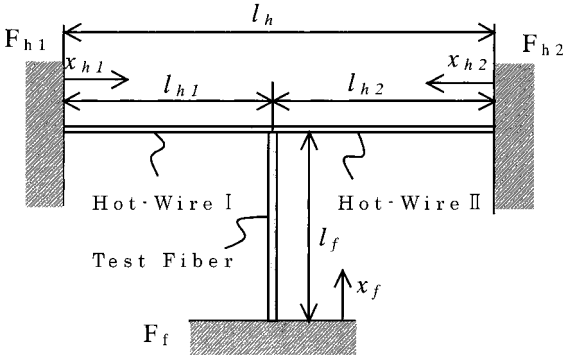

Fig. 1. Physical model.

Therefore, if we know exactly the relation between these quantities through the solutions of one-dimensional steady-state heat conduction along the hot wire and the test fiber, we could obtain the thermal conductivity of the test fiber by measuring the heat generation rate and average temperature of the hot wire. This method is applicable to both metallic and nonmetallic test fibers.

3. THEORETICAL ANALYSIS

3.1. Basic Equations and Boundary Conditions

As described above, both ends of the hot wire and one end of the test fiber are supported with the lead wires that have a high thermal conductivity and a large heat capacity compared to those of the hot wire and test fiber. Therefore, the temperature at both ends of the hot wire and one end of the test fiber can be assumed to maintain the initial temperature for the entire measurement. Assuming a uniform temperature in the radial direction for both the hot wire and the test fiber due to their small Biot number, the relevant basic equations are one-dimensional heat conduction equations expressed in dimensionless form as follows.

For hot wire I,

$$\frac{\partial \theta_{h1}}{\partial \mathrm{Fo}} = \frac{\partial^2 \theta_{h1}}{\partial X_{h1}^2} - 2\mathrm{Bi}\theta_{h1} + \frac{1}{R_c} \tag{1}$$

For hot wire II,

$$\frac{\partial \theta_{h2}}{\partial \mathrm{Fo}} = \frac{\partial^2 \theta_{h2}}{\partial X_{h2}^2} - 2\mathrm{Bi}\theta_{h2} + \frac{1}{R_c} \tag{2}$$

For the test fiber,

$$\frac{\partial \theta_f}{\partial \mathrm{Fo}} = \frac{1}{R_p}\frac{\partial^2 \theta_f}{\partial X_f^2} - 2\frac{R_c R_d}{R_p R_t}\mathrm{Bi}\theta_f \tag{3}$$

where the parameters R_c, R_p, R_t, and R_d are the ratios of thermal conductivity, thermal diffusivity, heat transfer coefficient, and radius of the hot wire and test fiber, respectively, and defined as

$$R_c = \frac{\lambda_h}{\lambda_f}, \qquad R_p = \frac{\alpha_h}{\alpha_f}, \qquad R_t = \frac{h_h}{h_f}, \qquad R_d = \frac{r_h}{r_f} \tag{4}$$

The dimensionless variables in Eqs. (1)–(3) are defined by

$$\theta = \frac{T - T_0}{q_v r_h^2/\lambda_f}, \quad \mathrm{Fo} = \frac{\alpha_h t}{r_h^2}, \quad \mathrm{Bi} = \frac{h_h r_h}{\lambda_h}, \quad X_{h1} = \frac{x_{h1}}{r_h}, \quad X_{h2} = \frac{x_{h2}}{r_h}, \quad X_f = \frac{x_f}{r_h} \tag{5}$$

Here q_v is the heat generation rate per unit volume and time, and Bi is the Biot number of the hot wire, which includes the effects of natural convection and radiation heat transfer.

The initial conditions are given by

Fo = 0:

$$\theta_{h1} = \theta_{h2} = \theta_f = 0 \tag{6}$$

and the boundary conditions are given by

$$\left.\begin{aligned} &\mathrm{Fo} > 0: \\ &\qquad \theta_{h1} = \theta_{h2} = \theta_f = 0; \qquad X_{h1} = X_{h2} = X_f = 0 \\ &\theta_{h1}\big|_{X_{h1}=L_{h1}} = \theta_{h2}\big|_{X_{h2}=L_{h2}} = \theta_f\big|_{X_f=L_f} \\ &\left.\frac{\partial \theta_f}{\partial X_f}\right|_{X_f=L_f} = -R_c R_d^2\left[\left.\frac{\partial \theta_{h1}}{\partial X_{h1}}\right|_{X_{h1}=L_{h1}} + \left.\frac{\partial \theta_{h2}}{\partial X_{h2}}\right|_{X_{h2}=L_{h2}}\right] \end{aligned}\right\} \tag{7}$$

3.2. Numerical Analysis of Transient Heat Conduction

The basic equations, Eqs. (1)–(3), are solved numerically by the finite difference method under the above initial and boundary conditions. Figure 2 shows the dimensionless temperature variations versus the logarithm of Fourier number for the different thermal conductivity ratios. The volumetric average temperature increases with an increase in Fourier number at the

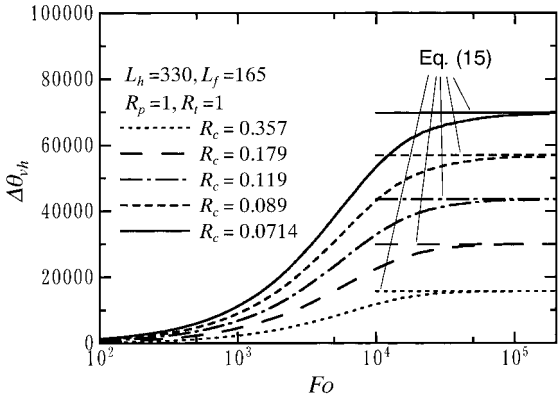

Fig. 2. $\Delta\theta_{vh}$ vs ln Fo at different thermal conductivity ratios R_c.

beginning and then reaches a steady-state temperature obtained by analytical solution and expressed by Eq. (15) at $\mathrm{Fo} = 10^5$, which corresponds to about 1 s in real time.

3.3. Analysis of Steady-State Heat Conduction

As shown in Fig. 2, it is easy to reach a steady state for the present heat transfer model. Therefore, to develop a new steady-state method for measuring the thermal conductivity of a fine fiber, the basic equations, Eqs. (1)–(3), without the unsteady terms are solved analytically. The general solutions for those equations may be written as follows:

$$\theta_{h1} = B_1 e^{-m_h X_{h1}} + B_2 e^{m_h X_{h1}} + \frac{1}{2R_c \mathrm{Bi}} \tag{8}$$

$$\theta_{h2} = C_1 e^{-m_h X_{h2}} + C_2 e^{m_h X_{h2}} + \frac{1}{2R_c \mathrm{Bi}} \tag{9}$$

$$\theta_f = D_1 e^{-m_f X_f} + D_2 e^{m_f X_f} \tag{10}$$

where the parameters m_h and m_f are defined as follows:

$$m_h = \sqrt{2\mathrm{Bi}}, \qquad m_f = \sqrt{2R_c R_d \mathrm{Bi}/R_t} \tag{11}$$

Considering boundary conditions as given in Eq. (7), the constants B_1, B_2, C_1, C_2, D_1, and D_2 are obtained as follows.

$$\left.\begin{aligned} B_1 &= \frac{2D_1 \sinh(m_f L_f) + U(1 - e^{m_h L_{h1}})}{2 \sinh(m_h L_{h1})} \\ B_2 &= -B_1 - U \\ C_1 &= \frac{2D_1 \sinh(m_f L_f) + U(1 - e^{m_h L_{h2}})}{2 \sinh(m_h L_{h2})} \\ C_2 &= -C_1 - U \\ D_1 &= \frac{S_2}{S_1} \\ D_2 &= -D_1 \end{aligned}\right\} \tag{12}$$

Here S_1, S_2, and U are defined as

$$\left.\begin{aligned} S_1 &= 2\left[\sinh(m_f L_f)\{\coth(m_h L_{h1}) + \coth(m_h L_{h2})\} + \frac{\cosh(m_f L_f)}{V}\right] \\ S_2 &= -U\left[\begin{matrix} e^{m_h L_{h1}}\{1 - \coth(m_h L_{h1})\} + e^{m_h L_{h2}}\{1 - \coth(m_h L_{h2})\} \\ + \coth(m_h L_{h1}) + \coth(m_h L_{h2}) \end{matrix}\right] \\ U &= \frac{1}{2R_c \mathrm{Bi}} \\ V &= \sqrt{R_c R_d^3 R_t} \end{aligned}\right\} \tag{13}$$

The nondimensional average temperature of the hot wire can be expressed as

$$\begin{aligned} \theta_{vh} &= \frac{1}{L_h} \int_0^{L_h} \theta_h \, dX \\ &= \frac{1}{L_{h1} + L_{h2}} \left(\int_0^{L_{h1}} \theta_{h1} \, dX_{h1} + \int_0^{L_{h2}} \theta_{h2} \, dX_{h2} \right) \end{aligned} \tag{14}$$

Substituting Eqs. (8) and (9) into Eq. (14), we can obtain the final form of the nondimensional average temperature for the hot wire as follows:

$$\theta_{vh} = \frac{1}{m_h(L_{h1} + L_{h2})} \left\{ \begin{matrix} -B_1 e^{-m_h L_{h1}} + B_2 e^{m_h L_{h1}} + B_1 - B_2 - C_1 e^{-m_h L_{h2}} \\ + C_2 e^{m_h L_{h2}} + C_1 - C_2 + \dfrac{m_h}{2R_c \mathrm{Bi}} (L_{h1} + L_{h2}) \end{matrix} \right\} \tag{15}$$

The solution corresponding to various conditions is shown in Fig. 2. When all parameters except for those including the fiber thermal conductivity λ_f are given, we can obtain the value of λ_f through measurement of the average temperature rise and heat generation rate of the hot wire by solving Eq. (15) with the Newton method.

4. UNCERTAINTY ANALYSIS

The uncertainty factors of the present measurements are summarized as follows.

4.1. Uncertainty of the Length of the Sample Fiber

The length of the sample fiber was measured with a micrometer having a resolution of 25 μm. According to the scattering range of several measurements, the uncertainty of length measurement is within 0.05 mm. When a sample fiber of about 6.5 mm in length is used, the uncertainty of the measured thermal conductivity caused by the uncertainty in the length of sample fiber is within 0.8%.

4.2. Uncertainty of the Diameter of the Sample Fiber

The diameter of the sample fiber was measured with a scanning electron microscope (SEM). For the platinum and copper wires, the uncertainty of measurement is 0.1%. For the carbon fibers, however, the uncertainty of measurement is about 1%, because the outline of SEM photographs is not clear. Therefore, the uncertainty of the measured thermal conductivity caused by the uncertainty in the diameter is estimated to be within 2%.

4.3. Uncertainty of the Position of the Junction Point

Similar to the uncertainty of the length measurement, the position measurement at the junction point is considered to be accurate to 0.05 mm. However, even for the same uncertainty of position measurement, the uncertainty of the measured thermal conductivity increases as the junction point departs from the center of the hot wire. Table I shows the corresponding uncertainty of the measured thermal conductivity for the various positions of the junction point.

Table I. Uncertainty in Thermal Conductivity Resulting from Junction Point Position

Sample	Junction point deviation from center of wire (mm)	Uncertainty of λ_f ($\pm$%)
Platinum wire	0.01	0.02
Copper wire	0.18	1.3
Carbon fiber		
(A-1)	0.28	2.0
(A-2)	0.01	0.2
(A-3)	0.04	0.5
(B-1)	0.50	3.5
(B-2)	0.28	2.0
(B-3)	0.19	1.4
(C-1)	0.15	1.1
(C-2)	0.20	1.4
(D-1)	0.20	1.4
(D-2)	0.28	2.0

4.4. Uncertainty of the Measurement of the Average Temperature Rise

Based on precalibration of the hot wire, the uncertainty of the average temperature rise is within 0.01 K. Therefore, the uncertainty of measured thermal conductivity caused by the uncertainty of the average temperature rise is about 0.4%. However, when the measurement is carried out at vacuum conditions, the temperature rise at the end junction part between the hot wire and the lead terminal should be considered. This temperature rise can be obtained by solving two-dimensional steady-state heat conduction for the lead terminal with a constant heat flux at the junction area between the hot wire and the lead terminal and with radiation heat transfer at the other surrounding surfaces. Based on the dimensions of the measuring probe, the numerical simulation shows about 0.02 K maximum temperature rise at the end junction area for the case of an average temperature rise of about 10 K. This end effect has been considered when we estimated the thermal conductivity of a sample fiber.

4.5. Uncertainty of Heat Transfer Coefficients of the Hot Wire and Sample Fiber

The heat transfer coefficients for the hot wire and sample fiber can be measured before the sample fiber is attached to the hot wire by using hot

wires of different diameters. As mentioned in our previous paper, when the heat transfer coefficient is less than 15 $W \cdot m^{-2} \cdot K^{-1}$, a 10% uncertainty of heat transfer coefficient results in less than 1% error in thermal conductivity. When the measurement is performed under vacuum conditions, the apparent heat transfer coefficient is less than 1 $W \cdot m^{-2} \cdot K^{-1}$. In this case, even for a 5% uncertainty caused by staining the junction part between the hot wire and the sample fiber with the platinum black glue, the uncertainty of the measured thermal conductivity is less than 0.6 %.

4.6. Uncertainty Caused by Thermal Conductance at the Junction Part

Generally, the effect of thermal conductance between the hot wire and the sample fiber increases as the thermal conductivity of the sample fiber increases. It is confirmed that when the platinum black glue is used as an adhesive agent, a 40% uncertainty in the thermal contact resistance results in less than 1% error in the thermal conductivity, because the total thermal resistance of the sample fiber is large compared with the contact resistance.

Besides the above six uncertainty factors, the uncertainty caused by the resistance measurements should also be considered. For the present probe, to measure the average temperature rise accurate to 0.01 K, a digital multimeter with 5.5 effective digits is required. In the present measurements, because two digital multimeters with 8.5 digits were used and their intrinsic fluctuations were limited to the last two digits, the uncertainty of the resistance measurements could be ignored. Therefore, the actual values of the overall uncertainty for the measured thermal conductivity are within 7%.

5. MEASUREMENTS

Figure 3 shows a schematic of the experimental setup. Figure 3a shows the details of the measuring probe. A short annealed Pt wire, 10.12 μm in diameter and 9.44 mm in length, is welded at both ends to a platinum lead wire 1.5 mm in diameter that is supported by a ceramic rectangular plate and connected with voltage and current lead wires. One end of the test fiber is attached at the center position of the hot wire with platinum black and the other end is attached to the platinum wire which has a diameter of 1.5 mm. Figure 3b shows the measurement system. It consists of a DC power supply and a voltage and current measuring and control system, that is, two digital multimeters (DMs) and a personal computer (PC). The power supply generates a constant current. The measurements were carried out automatically by using a sequential program and GPIB controlled with a personal computer.

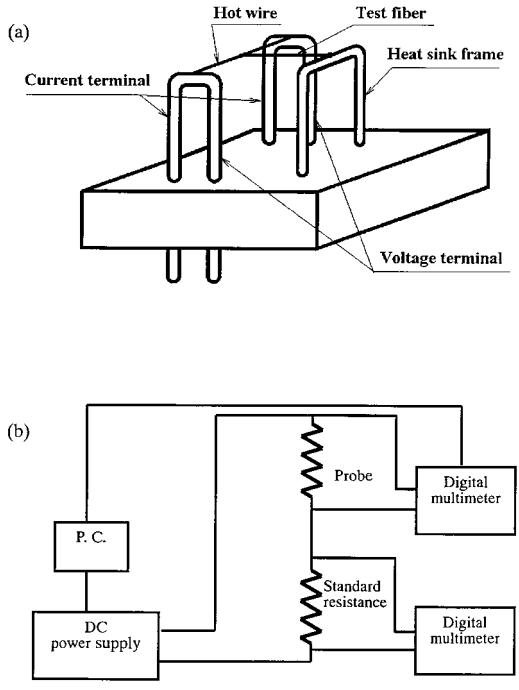

Fig. 3. Schematic of experimental setup. (a) Probe and test fiber; (b) Schematic of measuring system.

The average temperature T_v of the hot wire can be obtained by

$$T_v = \frac{1}{\beta}\left(\frac{R}{R_0} - 1\right) \tag{16}$$

where R and R_0 are the electrical resistance of the probe at the measuring temperature and 0°C, respectively, and where β is the temperature coefficient of its electrical resistance which is determined through a calibration.

The measuring procedure is simply summarized as follows. The setup of the probe and test fiber is first mounted on the bottom wall of a chamber, then the chamber is evacuated to 0.7 Pa. After the probe and chamber temperature becomes uniform and constant, a very small current, such as 0.1 mA, is supplied to the probe for 3 s to measure the initial wire temperature. Then a heating current of 3.4 mA is supplied to the probe. After the hot wire temperature becomes stable, the wire average temperature and heating rate can be measured. Therefore, the average temperature rise of the hot wire can be easily obtained by subtracting the initial wire temperature

from the wire average temperature. As described in Section 3.3, when all parameters such as the dimensions and heat transfer coefficient at 0.7 Pa were measured in advance, the fiber thermal conductivity λ_f can be estimated by solving Eq. (15).

Table II shows the dimensions and manufacturing conditions of the measured sample fibers. The platinum (purity, 99.98%) and copper (99.99%) wires were made by the Nilaco Corporation in Japan. The methylnaphthalene (mNP) carbon fibers (A-1)–(A-3) were made by the Institute of Advanced Material Study at Kyushu University, Japan. The carbon fibers (B-1)–(B-3), (C-1)–(C-2), and (D-1)–(D-2) were made by Nippon Mitsubishi Oil Corporation in Japan.

Table III shows the measured thermal conductivities and reference values. Each measured thermal conductivity is the average value of five measurements for the same sample fiber. For most measurements, the scatter of the measured thermal conductivity for the same sample fiber is within 1%, except for the carbon fiber (D-1), which shows differences of about 5%. For the platinum and copper wires, the measured values of the thermal conductivity are close to the reference values [12], which are the bulk values of the test samples. For the carbon fibers, the reference data [13] were estimated by measuring the thermal diffusivity of the bundle composite specimen of the fibers with the laser flash method.

Figure 4 shows a comparison between the measured data and the reference values obtained with other methods. For the platinum and copper wires, the present data agree well with the bulk values. For the carbon

Table II. Dimensions and Manufacturing Conditions of Sample Fibers

Sample	Diameter (μm)	Length (μm)	Notes
Platinum wire	10.12	6.33	Purity, 99.98%
Copper wire	22.24	6.43	Purity, 99.99%
Carbon fiber			
(A-1)	9.60	6.32	mNP Slit nozzle
(A-2)	9.86	7.40	400 rpm, air, 230°C
(A-3)	9.58	6.58	SHF, 2800°C × 5 min
(B-1)	6.64	7.76	$E = 870$ GPa
(B-2)	6.48	6.53	$G = 3.7$ GPa
(B-3)	6.94	6.40	
(C-1)	6.64	8.33	$E = 716$ GPa
(C-2)	6.64	5.85	$G = 3.9$ GPa
(D-1)	7.46	7.88	$E = 522$ GPa
(D-2)	7.08	6.58	$G = 4.1$ GPa

Table III. Measured Thermal Conductivity

Sample	T (K)	λ_f ($W \cdot m^{-1} \cdot K^{-1}$)	Ref. λ_f ($W \cdot m^{-1} \cdot K^{-1}$)	Difference (%)
Platinum wire	298	67.7	71.4	−5.2
Copper wire	298	410	398	3.0
Carbon fiber				
(A-1)	293	593	800	34.9
(A-2)	297	534	800	49.8
(A-3)	300	506	800	58.1
(B-1)	295	369	505	36.9
(B-2)	296	438	505	15.3
(B-3)	299	373	505	35.4
(C-1)	296	277	261	−5.8
(C-2)	296	211	261	23.7
(D-1)	296	116	133	14.7
(D-2)	296	130	133	2.3

fibers, the present data agree with the reference values for low values of the thermal conductivity. However, the difference between the two results increases with an increase in thermal conductivity. This difference is as large as 50%, especially for carbon fibers A. Although we cannot find any reasonable explanation why such a big difference between the two measurement methods exists, we can provide the following facts. First, the laser flash method can only directly measure the thermal diffusivity of the carbon fiber bundle. When the density and heat capacity of the carbon fiber bundle are further measured, the average thermal conductivity can be estimated. Second, there are practical difficulties in keeping all of the carbon fibers uniform in the composite specimen. Finally, the steady-state short-hot-wire method can directly measure the thermal conductivity of a single fiber and the values of the overall uncertainty for the measured thermal conductivity can be precisely estimated. This difference further demonstrates that the conventional method can give results for the thermal conductivity far from the actual value of the single fiber.

Table IV shows the measured thermal conductivities and electrical conductivities. The electrical resistance of the sample fiber can be measured directly with the four-point contact method and can be expressed as

$$R = \rho_0 \frac{l}{S} \tag{17}$$

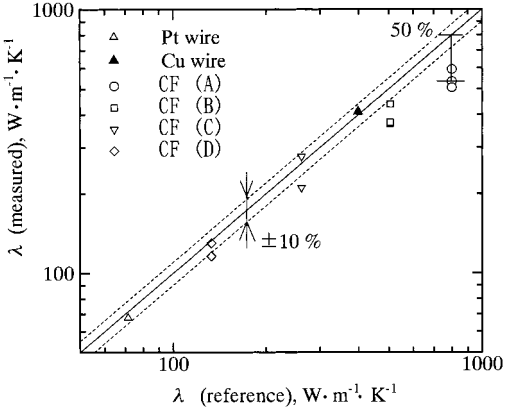

Fig. 4. Comparison between measured thermal conductivity and reference value.

where l and S are the length and cross-sectional area of the sample fiber, which are measured with a micrometer and SEM, respectively. ρ_0 is the electrical resistivity. The electrical conductivity is the inverse of ρ_0. The uncertainty of the measured electrical conductivity is estimated to be within 3%. The thermal conductivities of the carbon fibers (A), (B), (C), and (D) are the average values of the group data for the same type fiber shown in Table III.

Figure 5 shows the relation between the measured thermal conductivity and the electrical conductivity. The present data are close to the values from Refs. 14 and 15. For the higher-electrical conductivity region, a linear correlation between the thermal conductivity and the electrical conductivity can be obtained and expressed as

$$\lambda_f = 1261\sigma \tag{18}$$

Table IV. Measured Thermal Conductivity and Electrical Conductivity

Sample	λ_f ($W \cdot m^{-1} \cdot K^{-1}$)	σ ($MS \cdot m^{-1}$)
Carbon fiber		
(A)	544	0.428
(B)	393	0.413
(C)	244	0.205
(D)	123	0.158

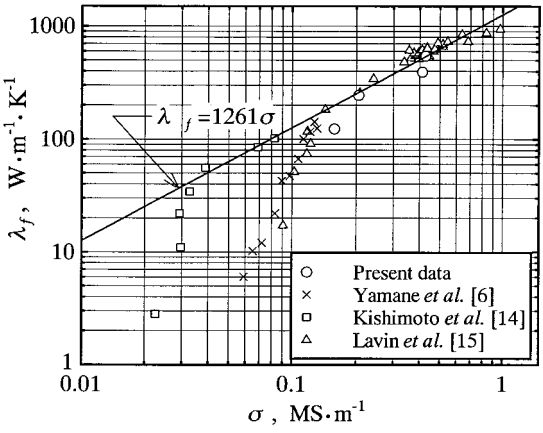

Fig. 5. Relation between thermal conductivity and electrical conductivity.

where σ is the electrical conductivity and λ_f is the thermal conductivity. In this region, the effects of the mean free path of phonons and relaxation time of electrons are considered to dominate thermal and electrical transport across grain boundaries of the crystal. Therefore, for the carbon fiber with a higher electrical conductivity, the thermal conductivity can be estimated by measuring its electrical conductivity. Further, as shown in Fig. 5, when the thermal conductivity λ_f is less than 30 $W \cdot m^{-1} \cdot K^{-1}$ [14] and 100 $W \cdot m^{-1} \cdot K^{-1}$ [6, 15], the slope of the thermal conductivity versus the electrical conductivity increases greatly. In this region, the effects of defects inside the crystal grains are considered to be dominant.

6. CONCLUSIONS

The short-hot-wire method has been used to measure the thermal conductivity of a single carbon fiber. The main conclusions are as follows.

1. Based on the uncertainty analysis, the short-hot-wire method under vacuum conditions can be used to measure the thermal conductivity of a single carbon fiber within an uncertainty of 7%.
2. A correlation between the thermal conductivity and the electrical conductivity for the fine carbon fiber at higher electrical conductivities has been proposed. This correlation can be used to predict the thermal conductivity by measuring its electrical conductivity.

3. Based on the crystal microstructure, the effects of the carbon fiber microstructures on the thermal conductivity can be limited by grain boundaries or by defects inside the grains.

NOMENCLATURE

Bi	Biot number
Fo	Fourier number
h	Heat transfer coefficient ($W \cdot m^{-2} \cdot K^{-1}$)
l_f	Length of test fiber (m)
l_h	Length of hot wire (m)
L_f	Dimensionless length of test fiber ($= l_f/r_h$)
L_h	Dimensionless length of hot wire ($= l_h/r_h$)
r	Radius (m)
R_c	Thermal conductivity ratio of hot wire and test fiber
R_d	Radius ratio of hot wire and test fiber
R_p	Thermal diffusivity ratio of hot wire and test fiber
R_t	Heat transfer coefficient ratio of hot wire and test fiber
S	Cross-sectional area of the test fiber (m^2)
t	Time (s)
T	Temperature (K)
T_0	Initial temperature (K)
x	Dimensional Cartesian coordinate (m)
X	Dimensionless Cartesian coordinate
θ	Dimensionless temperature
λ	Thermal conductivity ($W \cdot m^{-1} \cdot K^{-1}$)
α	Thermal diffusivity ($m^2 \cdot s^{-1}$)
σ	Electrical conductivity ($MS \cdot m^{-1}$)

Subscripts

f	Test fiber
h	Hot wire
v	Volumetric average

ACKNOWLEDGMENTS

The authors wish to acknowledge Professors I. Mochida and Y. Korai, both of the Institute of Advanced Material Study at Kyushu University, for providing carbon fiber samples and SEM and Nippon Mitsubishi Oil Corporation for providing carbon fiber samples and the thermal conductivity data obtained with the laser flash method.

REFERENCES

1. D. D. Edie, K. E. Robinson, O. Fleurot, S. P. Jones, and C. C. Fain, *Carbon* **32**:1045 (1994).
2. S. H. Yoon, Y. Korai, and I. Mochida, *Carbon* **31**:849 (1993).
3. G. Ventura, A. Bonetti, L. Lanzi, I. Peroni, A. Peruzzi, and G. Ponti, *Nucl. Phys. B, Proc. Suppl. (Netherlands)* **61B**:578 (1998).
4. H. Fujishiro, M. Ikebe, T. Kashima, and A. Yamanaka, *Jpn. J. Appl. Phys.* **36**:5633 (1997).
5. L. Piraux, J.-P. Issi, and P. Coopmans, *Measurement* **5**:2 (1987).
6. T. Yamane, S. Katayama, M. Todoki, and I. Hatta, *Therm. Conduct.* **22**:313 (1993).
7. R. E. Taylor, J. Jortner, and H. Groot, *Carbon* **23**:215 (1985).
8. L. F. Johnson, D. P. H. Hasselman, and K. Chyung, *J. Am. Ceram. Soc.* **70**:C135 (1987).
9. X. Zhang, S. Fujiwara, and M. Fujii, *Rep. Inst. Adv. Mater. Study Kyushu Univ.* **12**(1):29 (1998).
10. X. Zhang, S. Fujiwara, and M. Fujii, *Proceedings 19th Japan Symposium on Thermophysical Properties*, Fukuoka, p. 16 (1998).
11. X. Zhang, S. Fujiwara, and M. Fujii, *Proceedings 15th European Conference on Thermophysical Properties*, p. 216 (1999).
12. Japan Society of Thermophysical Properties, *Thermophysical Properties Handbook* (Yokendo, Tokyo, 1990).
13. Private communication, Nippon Mitsubishi Oil Corp. (1999).
14. I. Kishimoto, T. Baba, and A. Ono, *Therm. Conduct.* **24**:265 (1998).
15. J. G. Lavin, D. R. Boyington, J. Lahijani, B. Nysten, and J. P. Issi, *Carbon* **31**:1001 (1993).